**iScience, Volume *24***

## Supplemental information

# Personalized sleep-wake patterns aligned with circadian rhythm relieve daytime sleepiness

**Jaehyoung Hong, Su Jung Choi, Se Ho Park, Hyukpyo Hong, Victoria Booth, Eun Yeon Joo, and Jae Kyoung Kim**

**Data S1. Mathematical model description related to Figures 2-4 and STAR Methods.**

*Description of the original mathematical model of sleep-wake cycles*

To simulate the homeostatic sleep pressure and the circadian rhythm based on sleep-wake patterns and light exposure, our computational package adopted a physiologically-based mathematical model of sleep-wake cycles (Phillips et al., 2010; Skeldon et al., 2017; Swaminathan et al., 2017) (Figure S2). The variant of this model was already used for analyzing shift workers (Postnova et al., 2014). The variables and parameters used in the model are shown in Supplementary Tables S4 and S5 (see (Skeldon et al., 2017) for details). This model integrates the neuronal population model of the sleep-wake switch (Phillips and Robinson, 2008) and the human circadian pacemaker model (Kronauer et al., 1999). In the neuronal population model, mutual inhibition between wake-promoting monoaminergic (MA) neurons in the ascending arousal system and sleep-promoting neurons in the ventrolateral preoptic area (VLPO) of the hypothalamus are described by equations for their mean potential, $V_m$, and $V_v$, respectively:

$$\tau_m \frac{dV_m}{dt} = -V_m - \nu_{mv} Q_v + A_m, \quad (1)$$

$$\tau_v \frac{dV_v}{dt} = -V_v - \nu_{vm} Q_m - \nu_{vc} C + \nu_{vh} H + A_v, \quad (2)$$

where $\tau_m$ and $\tau_v$ denote the decay time of the MA and VLPO. The $\nu_{mv}$ and $\nu_{vm}$ determine the strength of the influence from VLPO to the MA and vice versa. The firing rates of the MA and VLPO neurons, $Q_m$ and $Q_v$, have sigmoidal relationship with their own potential:

$$Q_i = \frac{Q_{max}}{1+exp[\left(-\frac{V_i-\theta}{\sigma}\right)]} \quad (3)$$

where $i = m$ or $v$. The $Q_{max}$ and $\theta$ represent the maximum firing rate and the mean firing threshold, respectively, and $\sigma$ determines the width of the sigmoid. While the drive to MA (wake drive; $A_m$) is fixed, the drive to VLPO (sleep drive; $-\nu_{vc} C + \nu_{vh} H + A_v$,) depends on homeostatic sleep pressure $H$ (the level of somnogens such as adenosine) and the circadian rhythm of the master clock in the suprachiasmatic nucleus $C$. That is, as $H$ increases and $C$ decreases, the sleep drive increases. In this way, $H$ and $C$ control the transitions between sleep and wake (Figures 2A and S2). The homeostatic sleep pressure $H$ increases during wake and dissipates during sleep according to

$$\chi \frac{dH}{dt} = -H + \mu Q_m, \quad (4)$$

where $\mu$ and $\chi$ determine the production and the decay time of the homeostatic sleep pressure, respectively. The circadian rhythm $C$ is determined by

$$C = \frac{1}{2}(1 + c_x x + c_y y), \quad (5)$$

where $c_x$ and $c_y$ modulate the effect of the status of circadian pacemaker ($x$ and $y$) on the circadian rhythm. $x$ and $y$ are simulated by the circadian pacemaker model(Kronauer et al., 1999), which is described with a forced van der Pol oscillator with stiffness $\gamma$ and intrinsic period $\tau_c$:

$$\kappa \frac{dx}{dt} = \gamma \left(x - \frac{4x^3}{3}\right) - y(\left(\frac{24}{f\tau_c}\right)^2 + kB), \quad (6)$$

$$\kappa \frac{dy}{dt} = x + B. \quad (7)$$

This circadian pacemaker is entrained to external light signal which is transmitted from the retina to the master circadian clock in SCN via the retinohypothalamic tract. The transmitted light signal ($\tilde{I}$) is determined by the light exposure ($I$) and sleep-wake status. Specifically, the light exposure is attenuated by eyelids during sleep but not during wake:

$$\tilde{I} = \begin{cases} I, & \text{if } Q_m > Q_{th} \text{ (the wake state)} \\ 0, & \text{if } Q_m \leq Q_{th} \text{ (the sleep state)'} \end{cases} \quad (8)$$

where $Q_{th}$ determines the state of the model. This transmitted light signal ($\tilde{I}$) activates inactivated photoreceptors in the eye ($1 - n$) with the rate of activation $\lambda \alpha_0 \left(\frac{\tilde{I}}{I_0}\right)^p$ while activated photoreceptors ($n$) naturally return to inactivated photoreceptors with the rate of inactivation $\lambda \beta$:

$$\frac{dn}{dt} = \lambda(\alpha_0 \left(\frac{\tilde{I}}{I_0}\right)^p (1-n) - \beta n), \quad (9)$$

where the values of $\alpha_0$, $p$ and $I_0$ have been determined from experimental data (Kronauer et al., 1999). Proportional to inactivated photoreceptors $(1-n)$, the forcing of light intensity-dependent signals $B$ is determined according to:

$$B = G\alpha_0 \left(\frac{\tilde{I}}{I_0}\right)^p (1-n)(1-bx)(1-by) \quad (10)$$

where $(1-bx)(1-by)$ represents the sensitivity of the circadian system to light depending on phase.

The $C$ in Eq. (5) determines the thresholds of homeostatic sleep pressure, sleep threshold ($H^+$) and wake threshold ($H^-$):

$$H^+ = \frac{2.46 - A_v + \nu_{vc}C}{\nu_{vh}}, \text{ and} \quad (11)$$

$$H^- = \frac{1.45 - A_v + \nu_{vc}C}{\nu_{vh}}. \quad (12)$$

where 2.46 and 1.45 are the solutions of bifurcation in $V_v$ and $V_m$ (Puckeridge et al., 2011). When homeostatic sleep pressure is higher than the sleep threshold (i.e., sleep region; Figure S2B), MA is active while VLPO is silenced (Figure S2C), which triggers the transition from the wake to the sleep state. Similarly, when homeostatic sleep pressure is lower than the wake threshold (i.e., wake region; Figure S2B), the transition from sleep to wake state occurs. When homeostatic sleep pressure is between the sleep and the wake threshold (i.e., bistable region; Figure S2B), either sleep or wake is possible. The region below the sleep threshold is referred to as the potential wake region where the model would awake without effort which is interpreted as wake up without social constraint such as alarm clock (Skeldon et al., 2017).

*The modification of the mathematical model*

To investigate highly irregular sleep patterns of shift workers with indoor light profiles, we modified the original model as follows.

(1) Incorporation of realistic light attenuation: In the original model, light could not penetrate eyelids during sleep (Eq. (8)), so that $\tilde{I} = I$ during wakefulness ($Q_m > Q_{th}$) and $\tilde{I} = 0$ during sleep ($Q_m \leq Q_{th}$). We modified this attenuation to block 97% of the light rather than 100%, by

$$\tilde{I} = \begin{cases} I, \ if \ Q_m > Q_{th} \ (\text{the wake state}) \\ 0.03I, \ if \ Q_m \leq Q_{th} \ (\text{the sleep state}) \end{cases} \quad (13)$$

similar to (Swaminathan et al., 2017) because light exposure can still penetrate eyelids during sleep.

(2) Modification of parameters to match realistic light exposure with a sleep-wake cycle: In our data, the dark phase and sleep phase of shift workers are similar. However, the mathematical model with the original parameters cannot capture this pattern. Specifically, when the 16:8 LD cycle with 250 lux (typical indoor light intensity) and 0 lux are given for 120 days, the dark phase and sleep phase differ by more than 2 h. That is, for the dark phases between 22:00-6:00, 23:00-7:00 and 24:00-8:00 h, the sleep phases occur between 24:32-8:48, 25:32-9:48 and 26:32-10:48 h, respectively (Figures S3A, S3C, and S3E). Such a mismatch might be due to the fact that the original model was developed to explain what typical human adults do when they either do or do not have access to electric light. However, to analyze the data of shift workers, we had to match the dark phase and sleep phase. Thus, we changed the values of parameters determining the intrinsic period and phase of the circadian rhythm, and the ability of homeostatic sleep pressure to promote sleep which can change the sleep phase without large change in sleep duration (Phillips et al., 2010) : $\tau_c = 24.2$ h, $c_x = 0.47$, and $\nu_{vh} = 1.00$ mVnM$^{-1}$ to $\tau_c = 24.09$ h, $c_x = -0.16$, and $\nu_{vh} = 1.01$ mVnM$^{-1}$ (Table S5). With these modifications, the model simulated the sleep-wake cycle matching the realistic light exposure (Figures S3B, S3D and S3F).

With this modified parameter, we further needed an initial condition of the model to analyze sleep-wake patterns measured by wearable devices. For this, we assumed that one follows a baseline sleep-wake cycle before the measurement. The baseline sleep-wake cycle was chosen as sleep between 22:00-6:00 h because shift workers usually wake up at 6:00 h for the day shift and 8h is the typical recommended sleep duration of adults (Hirshkowitz et al., 2015). To simulate such a baseline sleep-

wake schedule with the modified parameters, the model simulated that sleep occurs between 22:04-6:10 h with light exposure of 250 lux between 6:00-21:42 h and 0 lux for the rest. The times of light off and sleep differed by 22 min, which was a reasonable difference since the mean sleep latency (the period between bedtime and sleep onset) of shift workers in SMC data was ~13 min±10 (Figure 1C).

(3) Incorporation of forced wakefulness and forced sleep: We modified the model to simulate the irregular sleep-wake cycle of shift workers by incorporating forced wakefulness and forced sleep because the original model could not simulate sleep when the model would naturally wake up (i.e., wake region) such as nap or long recovery sleep after the night shift. Furthermore, while the original model can simulate wake when the model would naturally fall asleep (i.e., sleep region) via wake effort (Skeldon et al., 2017), it was computationally challenging to simulate the complex sleep-wake patterns of shift workers as a dramatic change in the amount of wake effort drive needs to be tracked. Thus, we adopted a relatively simple approach, the forced wakefulness from the previous study (Phillips and Robinson, 2008; Postnova et al., 2014) (Figure S4). Specifically, we first saved the level of wake- and sleep-promoting neurons when MA had its highest value and VLPO was suppressed during the baseline sleep-wake pattern (Figures S3C and S3D). Then, the activity of MA and VLPO was simply kept at this pre-calculated level during the forced wakefulness (Figure S4). Similarly, forced sleep was simulated by simply keeping the MA suppressed and the VLPO activated at a pre-calculated level when MA had its lowest value during the baseline sleep-wake pattern (Figure S4). When the model was in the bistable region between sleep and the wake threshold, the transition between sleep and wake was simply made by temporally changing the activity of MA and VLPO rather than using forced wakefulness or forced sleep (Figure S5). While we used the forced wakefulness and sleep for simplicity, wake and sleep efforts can also be used to calculate the necessary sleep and thus CSS.

(4) Incorporation of chronotype: according to chronotype of shift workers measured by MEQ, we used different values of the parameter $\tau_c$ determining intrinsic period of the circadian rhythm similar to the previous study (Swaminathan et al., 2017): 24.09 h for intermediate type, 24.35 h for evening type and 23.85 h for morning type. However, for two participants of SMC data who had MEQ score 41 (threshold score of evening type), we kept $\tau_c = 24.09$ h because MEQ score was too close with intermediate type to change the intrinsic period of the circadian rhythm (Baehr et al., 2000). Future work can consider the gradual change of $\tau_c$ depending on MEQ score.

*Calculation of the duration of circadian necessary sleep and CSS*

For each main sleep episode, the duration of circadian necessary sleep was determined as the duration from sleep onset to the time when the homeostatic sleep pressure becomes lower than the sleep threshold. To calculate the duration of circadian necessary sleep, the light exposure measured by the actiwatch and the light exposure of 0 lux were used during sleep and wake, respectively. If sleep onset of the main sleep episode occurs before reaching the sleep threshold (i.e., forced sleep) and never reaches the sleep region during the sleep episode, the duration of circadian necessary sleep is zero, which is unrealistic. In this case, we allow for the model to be in wakefulness without the forced sleep under the light exposure of 250 lux until reaching the sleep threshold. Then, we calculated the duration of circadian necessary sleep (i.e., how long it takes for the homeostatic sleep pressure to become lower than the sleep threshold).

If the sleep duration of a main sleep episode (i.e., time from sleep onset to sleep offset−WASO) is longer or equal than the duration of circadian necessary sleep, the main sleep episode is determined as the circadian sufficient sleep. On the other hand, if the sleep duration of a main sleep episode is shorter than the duration of the circadian necessary sleep, which includes the absence of the main sleep episode, the main sleep episode is determined as a circadian insufficient sleep. Then, the fraction of circadian sufficient sleeps in total sleep days during the study period was calculated as the CSS.

**Data S2. Manual for computational package related to Figure 3 and STAR Methods.**

As described in STAR Methods, we developed the computational package which analyzes sleep-wake patterns. The MATLAB codes of the computational package are available at: https://github.com/Mathbiomed/CSS. The computational package can be used as followed (Figure S6).

Step 1. *Fill in the 1st column of 'Input1_sleep_light.csv'* (Figure S6A). The $n^{th}$ row contains 'Sleep' for sleep status and 'Wake' for wake status at the $n^{th}$ epoch. Note that the 1st epoch must begin with 'Wake'. Users who use the Actiwatch just need to change 'REST-S' of 'Interval Status' to 'Sleep' and 'REST' and 'ACTIVE' to 'Wake' after processing to avoid any missing period (see STAR Methods). Users who do not use the Actiwatch can also easily fill in the 1st column by using 'Sleep_make.m'. To run 'Sleep_make.m', users need to fill in 'Input1_sleep.csv' and locate it in the same folder with 'Sleep_make.m'. Specifically, users need to fill in date of sleep onset (year-month-day), sleep onset (h), date of sleep offset and sleep offset of the $n^{th}$ sleep episode in the $n^{th}$ row of the 1st, 2nd, 3rd and 4th column of 'Input1_sleep.csv', respectively (see the example file for the details). Then, after running 'Sleep_make.m', 'Maked_sleep.csv' will be created, which can be used to fill in the 1st column of 'Input1_sleep_light.csv'. The duration of the epoch is automatically chosen as 2 min as default and the starting time of sleep-wake state is provided by the 'Sleep_make.m'.

Step 2. *Fill in the 2nd column of 'Input1_sleep_light.csv'* (Figure S6A). The $n^{th}$ row contains the light exposure (lux) of users at each epoch (see the example file for the details). If users did not measure light exposure, it is recommended to fill in 250 lux at wake status and 0 lux at sleep status.

Step 3. *Fill in the 1st column of 'Input2_WASO_main.csv'* (Figure S6B). Specifically, users need to fill in WASO (min) of the $n^{th}$ sleep episode at the $n^{th}$ row of the 1st column (see the example file for the details). Users who use the Actiwatch can easily do this by using 'Waso_make.m'. To run 'WASO_make.m', users first need to specify the value of time_interval in the 1st line of the 'WASO_make.m' according to the duration of the epoch (min). Then, users need to fill in the 1st column and 2nd column of 'Input2_waso.csv' with 'sleep/wake' reading supplied by the Actiwatch after processing to avoid any missing period (see STAR Methods) and the 1st column of 'Input1_sleep_light.csv' which was made at Step1, respectively. Then, after locating them in the same folder, running 'WASO_make.m' will create 'Maked_WASO.csv', which can be used as the 1st column of 'Input2_WASO_main.csv'.

Step 4. *Fill in the 2nd column of 'Input2_WASO_main.csv'* (Figure S6B). Specifically, fill in the $n^{th}$ row with 'M' if $n^{th}$ sleep episode is the main sleep episode and 'N' if not

Step5. *Edit 'CSS_package.m'* (Figure S6C). Users need to specify the value of time_interval, time_start, and tau_c in the code. Specifically, time_interval is the duration of epoch (min) and time_start is the starting time (h) of sleep-wake state. tau_c = 23.85 h, 24.09 h, and 24.35 h if users are morning, intermediate, and evening types, respectively.

Step7. *Run 'CSS_package.m'* (Figure S6D). The folder named 'Output' will be automatically created, which includes three output files:

(1) 'H_C.png': The homeostatic sleep pressure and the circadian rhythm of users.

(2) 'CSS.png': The comparison between the predicted duration of circadian necessary sleep and the actual sleep duration of users for each main sleep episode.

(3) 'CSS.csv': The $n^{th}$ row of the 1st and 2nd columns contain the predicted duration of circadian necessary sleep and the actual sleep duration of $n^{th}$ main sleep episode, respectively. The $n^{th}$ row of the 3rd column contains 'S' and 'I' if the $n^{th}$ main sleep episode is circadian sufficient and circadian insufficient, respectively. The fourth column describes daily change of CSS.

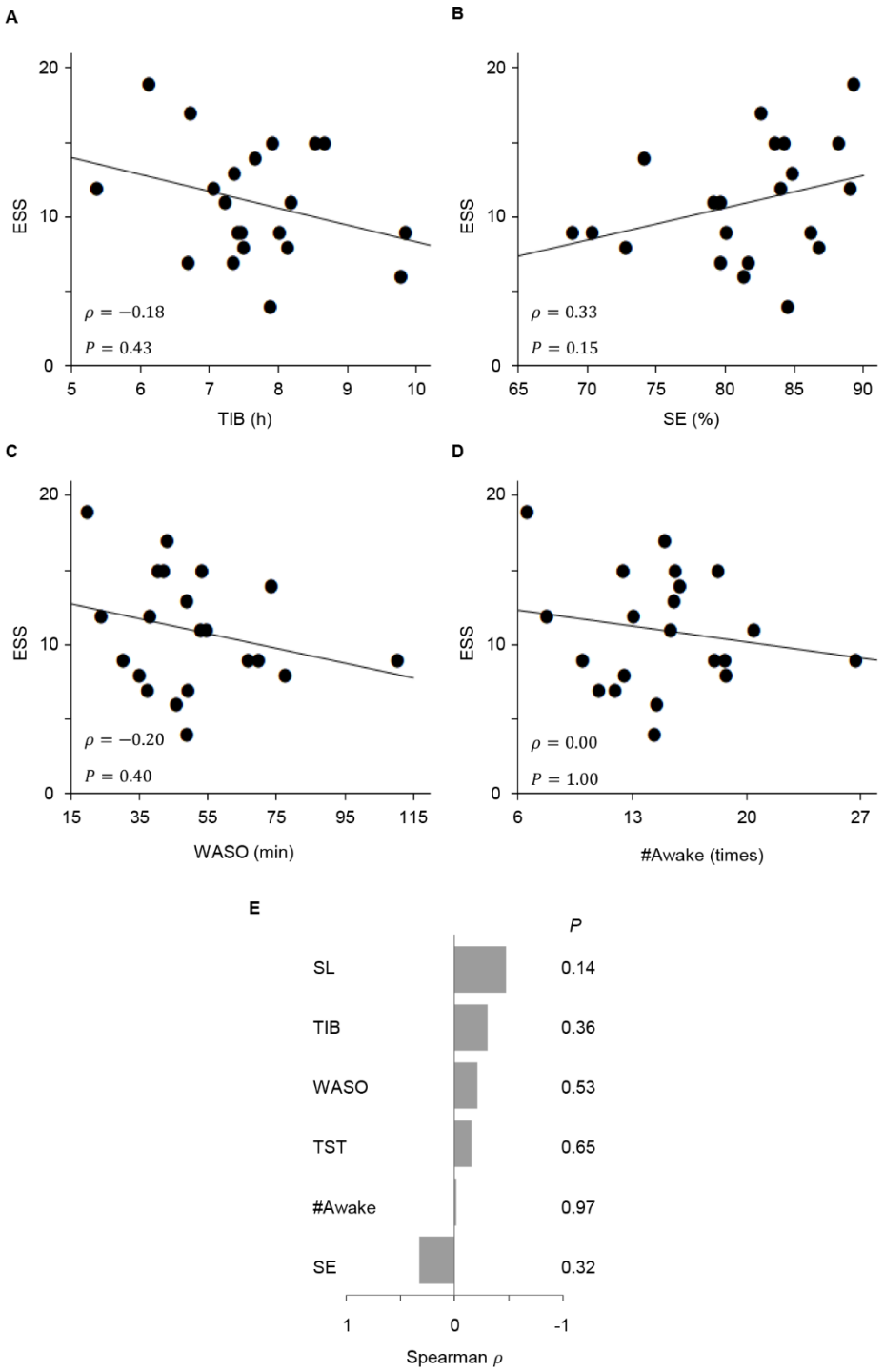


**Figure S1**. **No significant correlation was found between standard sleep parameters and daytime sleepiness of shift workers, related to Figure 1. (A-D)** Scatter plots of TIB (A), SE (B), WASO (C), #Awake (D) versus ESS of shift workers. The mean±SD of such parameters are 7.68 h±1.05, 81.56 %±5.84, 50.90 min±20.53, 14.96 times±4.51, respectively. Similar to TST (Figure 1B) and SL (Figure 1C), none of them had a significant correlation with ESS. The line represents the least-square fitting line. $\rho$ and $P$ denote the Spearman's rank correlation coefficient and *p* value of Spearman's rank correlation test, respectively. (**E**) No significant correlation was found between standard sleep parameters and daytime sleepiness of shift workers despite controlling covariates, such as age, clinical experience, marital status, BMI, caffeine & alcohol intake, the number of day, evening, and night shifts.

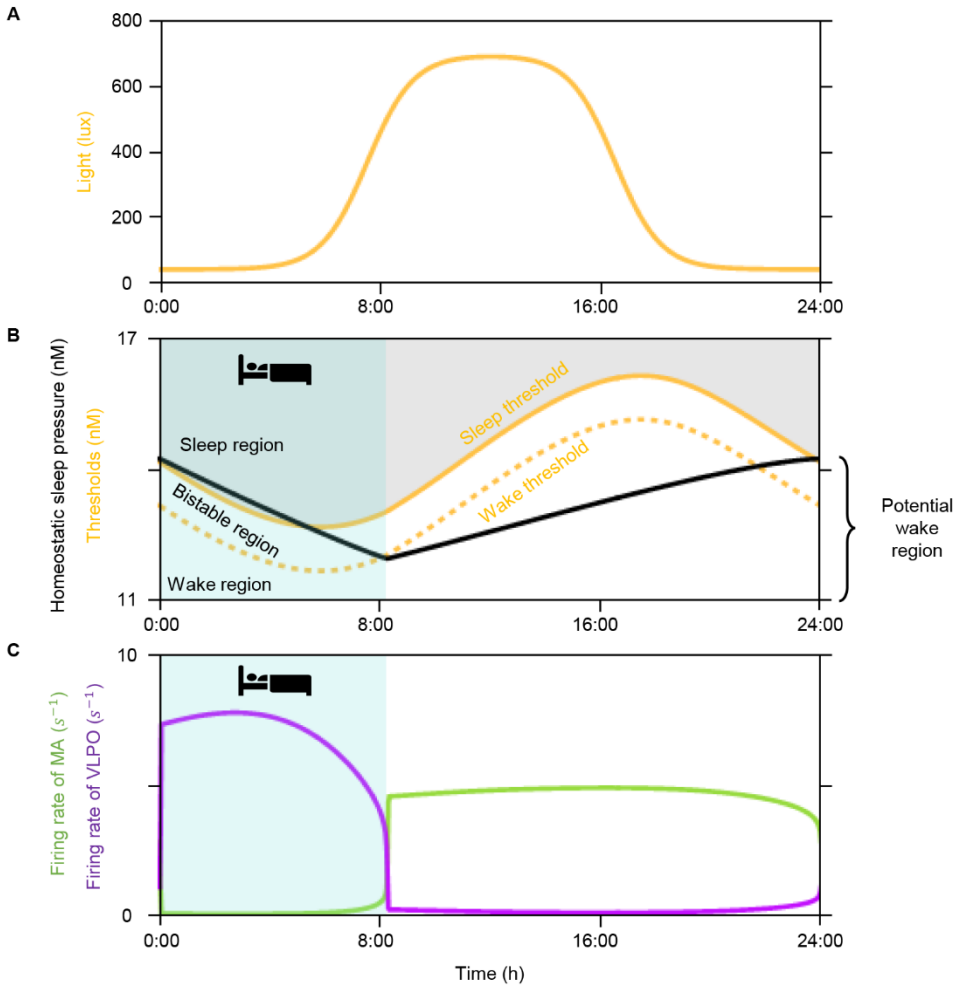


**Figure S2. The sleep-wake behavior of the mathematical model was determined by the interaction between homeostatic sleep pressure and sleep and wake thresholds, related to Figure 2 and STAR Methods. (A)** The light exposure which gives daylight durations (~700 lux) of approximately 12 h centered on noon (yellow line). **(B)** With such light exposure, the original mathematical model of sleep-wake cycle simulates the sleep-wake pattern of which sleep occurs between 00:04 h and 08:12 h (blue shades). Such a sleep-wake pattern is determined by the interaction between homeostatic sleep pressure (black line) and the circadian rhythm, which determines the sleep (yellow solid line) and wake thresholds (yellow dotted line). When the homeostatic sleep pressure reaches the sleep region (i.e., passes above the sleep threshold; gray region), the model would naturally fall asleep. Conversely, when the homeostatic sleep pressure reaches the wake region (i.e., passes below the wake threshold), the model would naturally wake up. When homeostatic sleep pressure reaches the bistable region (i.e., the region between the sleep and wake thresholds), both sleep and wake are available. The potential wake region is defined as the region below the sleep threshold where the model would awake without effort (i.e., bistable region+wake region). **(C)** When the homeostatic sleep pressure reaches the sleep region, the firing rate of sleep-promoting neurons in the ventrolateral preoptic area (VLPO; purple line) increases while the firing rate of wake-promoting monoaminergic (MA) neurons (green line) decreases, which triggers the transition from wake to sleep. Similarly, when the homeostatic sleep pressure reaches the wake region, the firing rate of VLPO (purple line) decreases while the firing rate of MA (green line) increases, which triggers the transition from sleep to wake.

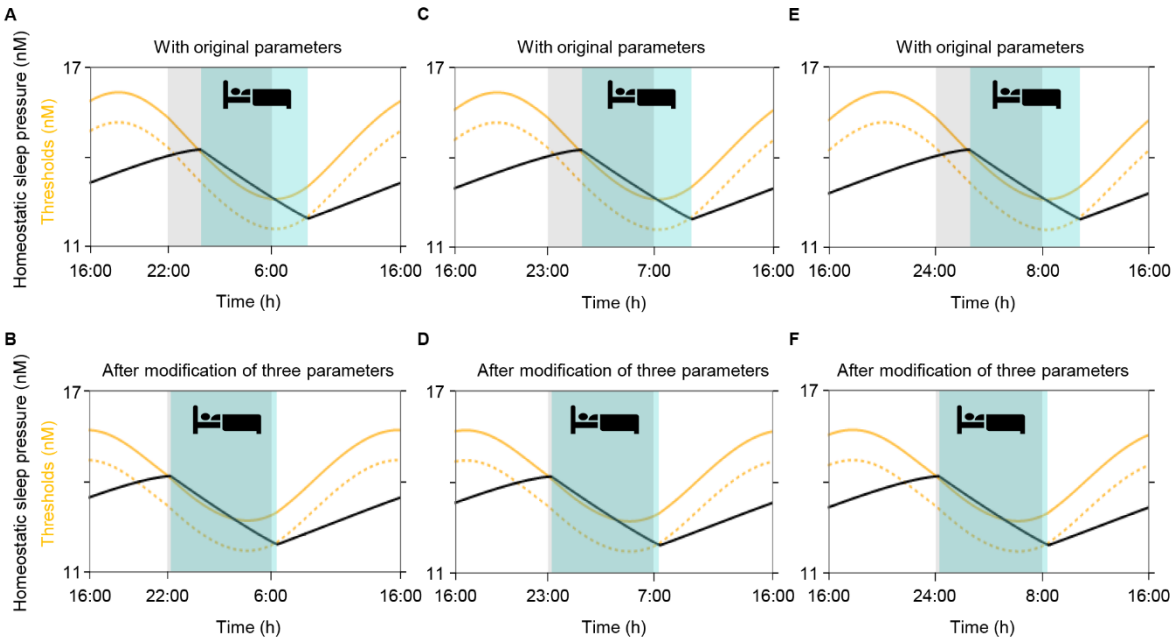


**Figure S3. Parameter values of the mathematical model were modified to match the simulated sleep-wake cycles with the realistic light exposures, related to Figure 2 and STAR Methods.** (**A-F)** For 120 days under the LD cycle with varying dark phases between 22:00-6:00 h (A, B), 23:00-7:00 h (C, D), and 24:00-8:00h (E, F), the sleep-wake cycles were simulated using the original parameters (A, C, E) and the modified parameters (B, D, F). The dark phases and the sleep phases simulated using the original parameters differ by more than 2 h (A, C, E). On the other hand, such a large mismatch no longer occurred when the modified parameters were used (B, D, F).

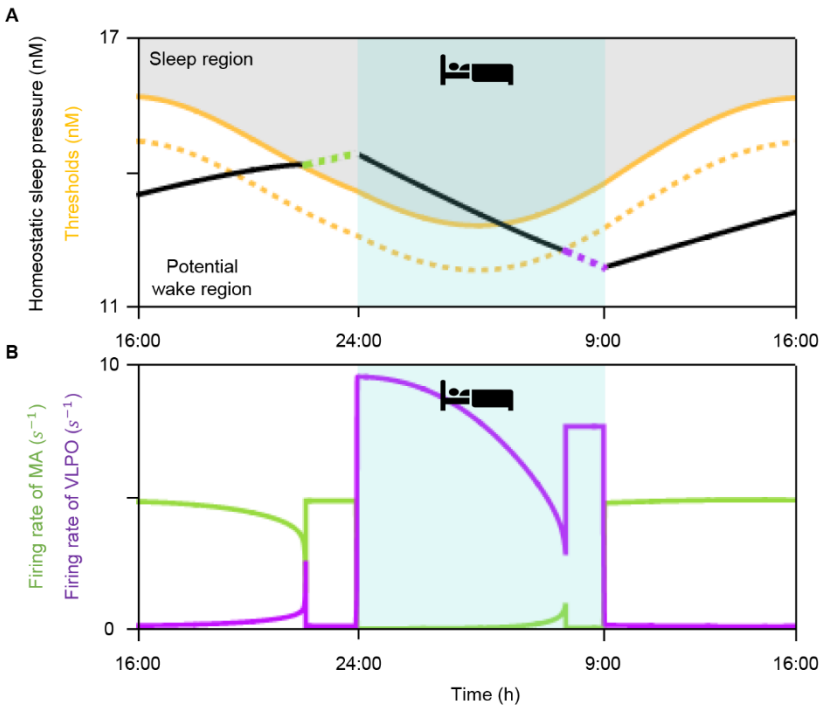


**Figure S4. Incorporation of forced wakefulness and sleep into the mathematical model by keeping MA and VLPO at their wake- and sleep-level, related to Figure 2 and STAR Methods. (A** and **B)** To simulate the sleep (blue shade) that is not aligned with the circadian rhythm, the mathematical model needs to simulate the wake and sleep when the model would naturally fall asleep and wake up, respectively (A). To this end, we incorporated forced wakefulness and forced sleep into the model. When the homeostatic sleep pressure reached the sleep region (A), we kept the firing rate of MA (green line; B) and VLPO (purple line; B) as the pre-calculated wake-level when MA had its highest firing rate during the baseline sleep-wake pattern : $(V_m, V_v) = (1.08, -10.15), (1.09, -10.19)$ and $(1.09, -10.22)$ for morning, intermediate and evening types, respectively. In this way, the model was able to simulate wake despite that it would naturally fall asleep (green dotted line; A). Similarly, when the homeostatic sleep pressure reached the wake region, we kept the firing rate of MA (green line; B) and VLPO (purple line; B) at the pre-calculated sleep-level when MA had its lowest firing rate during the baseline sleep-wake pattern : $(V_m, V_v) = (-12.42, 2.52), (-12.57, 2.55)$ and $(-12.63, 2.56)$ for morning, intermediate and evening types, respectively. As a result, the model was able to simulate sleep despite that it would naturally wake (purple dotted line; A).

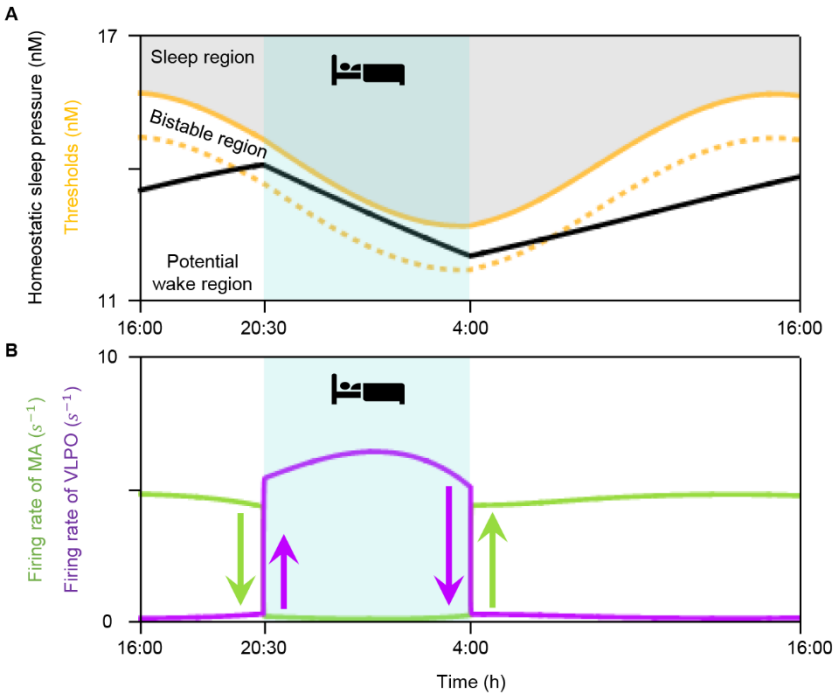


**Figure S5. When the mathematical model was in the bistable region, the transition between sleep and wake was made by instantaneous change of the firing rate of MA and VLPO, related to Figure 2 and STAR Methods. (A** and **B)** When the mathematical model was in the bistable region (A), the transition between sleep and wake was made without forced wakefulness or forced sleep (Figure S4). Specifically, it was made by instantaneously changing the firing rate of MA and VLPO at the sleep onset to the value at the sleep-level (i.e., decrease firing rate of MA (green arrow) and increase VLPO (purple arrow; B), the transition from sleep to wake was simulated. Similarly, the instantaneous change of the firing rate of MA and VLPO at the sleep offset to the value at the wake-level (i.e., increase the firing rate of MA (green arrow) and decrease VLPO (purple arrow; B) simulated the transition from wake to sleep. Specifically, the transition from wake to sleep and vice versa was made by instantaneously changing $V_m = -4.78$ and $V_v = 0$ at sleep onset and $V_m = -0.12$ and $V_v = -4.66$ at sleep offset, respectively. Such values of $V_m$ and $V_v$ were chosen as the solutions of bifurcation in $V_v$ and $V_m$ (Puckeridge et al., 2011).

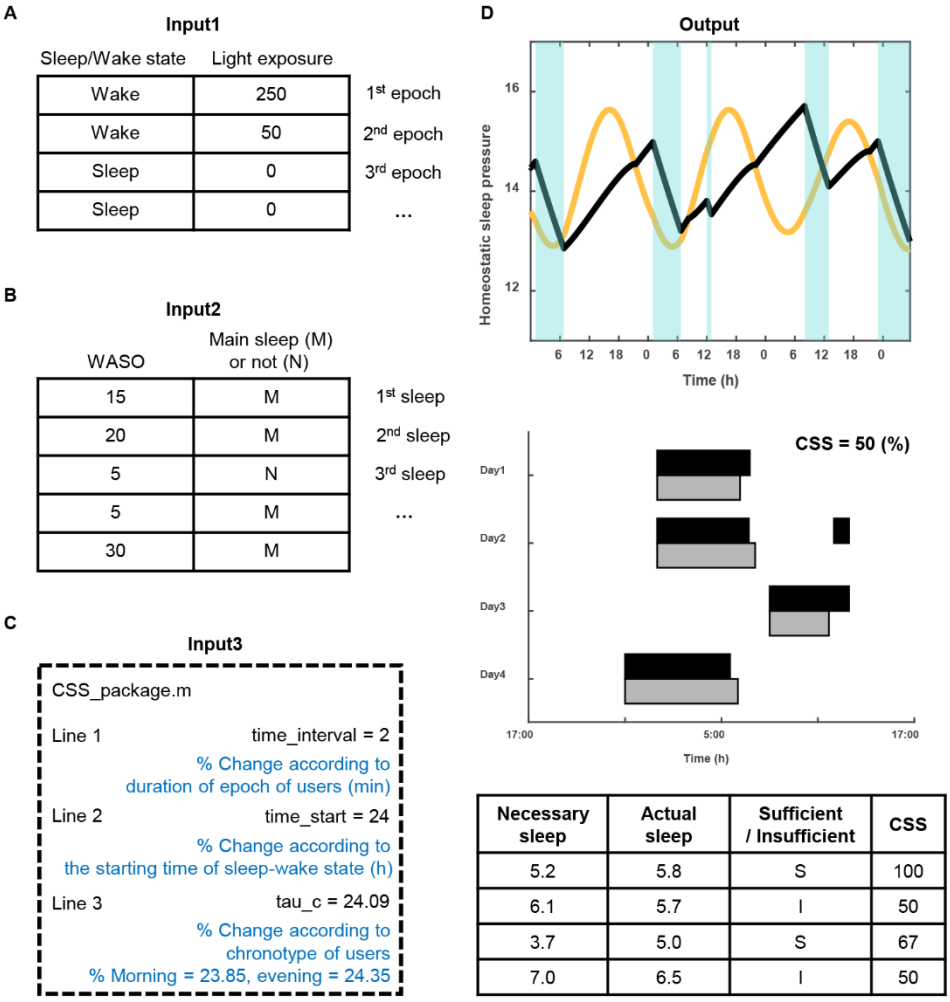


| Necessary sleep | Actual sleep | Sufficient / Insufficient | CSS |
|---|---|---|---|
| 5.2 | 5.8 | S | 100 |
| 6.1 | 5.7 | I | 50 |
| 3.7 | 5.0 | S | 67 |
| 7.0 | 6.5 | I | 50 |

**Figure S6. The schematic description of the computational package, related to Figure 3 and STAR Methods. (A)** The file input1 contains sleep/wake state and light exposure at each epoch. **(B)** The file input2 contains the WASO of each sleep episode and specification for main sleep. **(C)** To run the computational package, the duration of the epoch, the starting time of the sleep-wake state, and chronotype of users need to be determined. **(D)** The three output files are created after running the computational package. The 1st file illustrates variations of homeostatic sleep pressure and the circadian rhythm according to sleep-wake pattern and light exposure of users (top). The 2nd file includes the comparison between predicted duration of circadian necessary sleep (gray bar; middle) of each main sleep episode and actual sleep duration (black bar; middle) of each sleep episode. The 3rd file includes the analysis of sleep: whether each main sleep episode is circadian sufficient sleep (S) or circadian insufficient sleep (I), and how the circadian sleep sufficiency (CSS) changes (bottom).

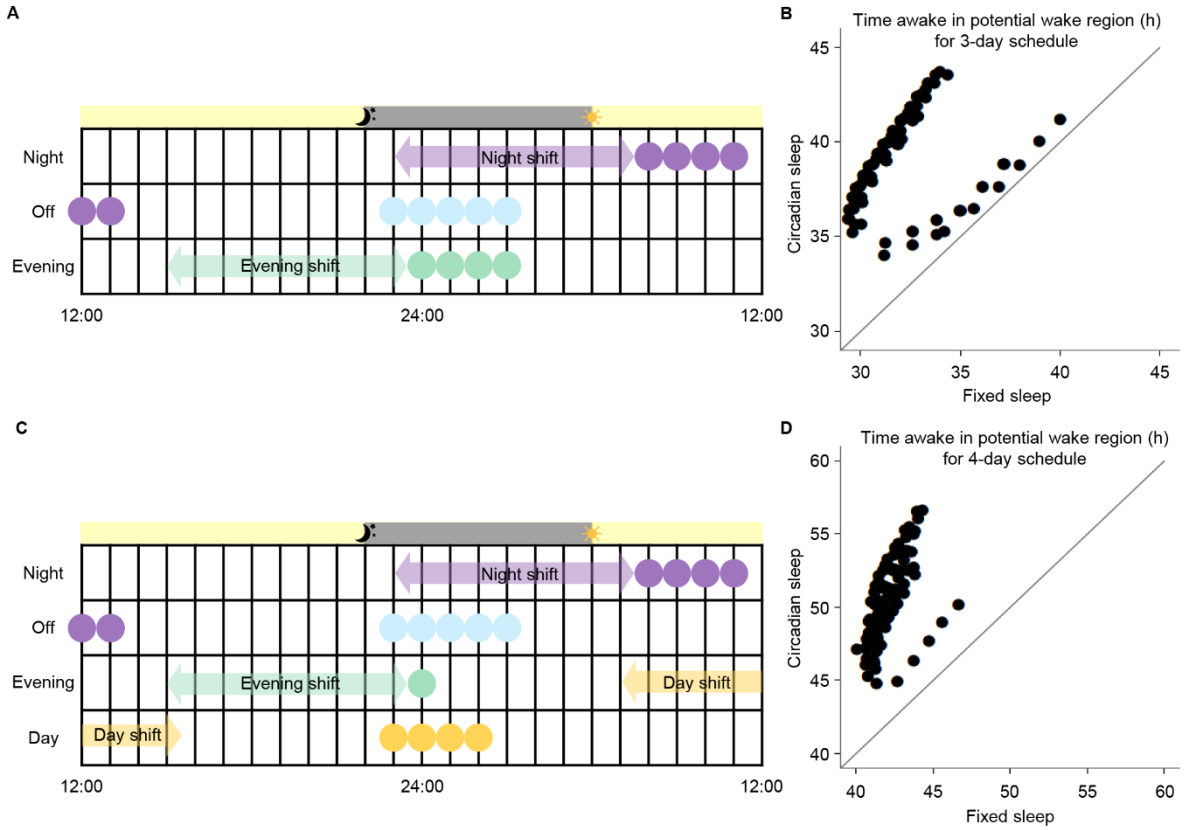


**Figure S7. Sleep-wake patterns aligned with the circadian rhythm increase the time awake in the potential wake region regardless of the sleep onset times during the shift schedule and the lengths of the shift schedule, related to Figure 4. (A)** Potential sleep onset times for the 3-day shift schedule considering the shift schedule (evening shift, 15:00-23:30 h; night shift, 23:00-07:30 h). For instance, after the evening shift, the sleep onset time should be after 23:30 h since the evening shift finishes at 23:30 h. In total, we considered 120 scenarios of different sleep onset times ($6 \times 5 \times 4$) for three days. **(B)** For all of these scenarios, we fixed the sleep duration as 6 h regardless of the sleep onset times to simulate the fixed sleep, leading to TST=6h. On the other hand, to simulate the circadian sleep, we optimally adjusted the sleep duration according to the sleep onset time, leading to the maximal CSS. Specifically, the day after the night shift, we optimally chose either 4-, 4.5- or 5-h sleep episodes. Then, for the other days, we chose the duration of the sleep episode while maintaining TST=6 h. The circadian sleep simulation leads to longer times awake in the potential wake region (up to 10 h) compared to the fixed sleep simulation. Here, the model was simulated for 120 days under the same schedule to reach a stable and entrained sleep-wake cycle. **(C)** Potential sleep onset times for the 4-day shift schedule considering the shift work schedule (day shift, 07:00-15:30 h; evening shift, 15:00-23:30 h; night shift, 23:00-07:30 h). For instance, after the evening shift, the sleep onset time should be after 23:30 h since the evening shift finishes at 23:30 h. Similarly, before the day shift, the sleep onset time should be before 24:30 h to make the sleep offset time before 7:00 h. In total, we considered 120 scenarios of different sleep onset times ($6 \times 5 \times 1 \times 4$) for four days. **(D)** For all of these scenarios of the 4-day shift schedule, the circadian sleep simulation leads to longer times awake in the potential wake region (up to 13 h) compared to the fixed sleep simulation.

| Variables | Subjects (n=21) | mean±SD | Range |
|---|---|---|---|
| Age, y | | 32.19±4.37 | 25~41 |
| Marital status | | | |
| Single | 10(47.6) | | |
| Married | 11(52.4) | | |
| Clinical experience, y | | 8.45±4.07 | 1.0~15.9 |
| Body mass index, kg/m$^2$ | | 20.20±2.57 | 16.0~28.3 |
| Caffeine consumption, cups/day | | 1.53±0.97 | 0.1~4.5 |
| Alcohol intake | 11(52.4) | | |
| Comorbid health problem | | | |
| Gastrointestinal trouble | 1(4.8) | | |
| Irregular menstruation | 7(33.3) | | |
| Insomnia severity index (ISI) | | 12.33±4.39 | 4~21 |
| Epworth sleepiness scale (ESS) | | 10.95±3.89 | 4~19 |
| Excessive daytime sleepiness (EDS; ESS>10) | 11(52.4) | | |
| Chronotype (M:I:E) | 2(9.5):16(76.2):3(14.3) | | |

**Table S1. Demographics of SMC data, related to Figure 1 and STAR Methods.** Percent is calculated over a total of 21 nurses. Chronotype is determined by MEQ: M, I, and E represent morning (Subject with scores above 58), intermediate (42-58) and evening types (below 42), respectively.

| Parameters | ρ | P |
|---|---|---|
| Skeldon et al., 2017<br>(With the indoor light profile) | $-0.3139$ | $0.1658$ |
| Skeldon et al., 2017<br>(With the natural light profile) | $-0.3129$ | $0.1672$ |

**Table S2. The correlation between the CSS and daytime sleepiness when the mathematical model with the original parameters was used, related to Figure 3.** The CSS was calculated with the mathematical model with the original model parameters (Skeldon et al., 2017) after the initial entrainment with either the indoor light profile we used (Figure S2) or the natural light profile used in the previous paper (Skeldon et al., 2017). $\rho$ and $P$ denote the Spearman's rank correlation coefficient and the p value of Spearman's rank correlation test, respectively.

| Imputed light intensity for missing period (lux) | Mean change of CSS (%) | ρ |
|---|---|---|
| 100 | 2.72 | -0.43 |
| 200 | 1.02 | -0.51* |
| 300 | 0.34 | -0.50* |
| 400 | 0.34 | -0.50* |
| 500 | 0.68 | -0.46* |
| 600 | 0.68 | -0.46* |
| 700 | 1.02 | -0.47* |

**Table S3. CSS depending on the imputed light intensity for missing data, related to Figure 3.** As the imputed light intensity was chosen between 100 and 700 lux instead of 250 lux (default value of our package) for missing data, the CSS changes little on average (<2.72%) and thus the correlation between CSS and daytime sleepiness change little. ρ denotes the Spearman's rank correlation coefficient Sp earman's rank correlation test, respectively. *P<0.05.

| Name | Symbol |
|---|---|
| The mean potential of MA | $V_m$ |
| The mean potential of VLPO | $V_v$ |
| The homeostatic sleep pressure | $H$ |
| The auxiliary variable of the circadian system | $x$ |
| The pacemaker activity of the circadian system | $y$ |
| The fraction of activated photoreceptors | $n$ |

**Table S4. The variables of the mathematical model, related to Figure 3 and STAR Methods.**

| Sleep/wake regulation parameters | | | |
|---|---|---|---|
| $\boldsymbol{\nu_{vh}}$ | **1.01 mVnM$^{-1}$** | $Q_{max}$ | 100 s$^{-1}$ |
| $Q_{th}$ | 1 s$^{-1}$ | $\theta$ | 10 mV |
| $\sigma$ | 3 mV | $\tau_m$ | $\frac{1}{360}$ h |
| $\tau_v$ | $\frac{1}{360}$ h | $\chi$ | 45 h |
| $\mu$ | 4.2 nMs | $\nu_{mv}$ | 1.8 mVs |
| $\nu_{vm}$ | 2.1 mVs | $\nu_{vc}$ | 3.37 mV |
| $A_m$ | 1.3 mV | $A_v$ | −10.2 mV |
| **Circadian parameters** | | | |
| $\boldsymbol{\tau_c}$ | **23.85 h (M)**<br>**24.09 h (I)**<br>**24.35 h (E)** | $\boldsymbol{c_x}$ | **−0.16** |
| $\alpha_0$ | 0.16 | $\beta$ | 0.013 |
| $p$ | 0.6 | $I_0$ | 9500 lux |
| $\lambda$ | 60 h$^{-1}$ | $G$ | 19.9 |
| $b$ | 0.4 | $\gamma$ | 0.23 |
| $\kappa$ | $\frac{12}{\pi}$ h | $k$ | 0.55 |
| $f$ | 0.99669 | $c_y$ | 0.8 |

**Table S5. Parameters of the mathematical model, related to Figure 3 and STAR Methods.** The values of parameters were taken from the original mathematical model except for $v_{vh}$, $\tau_c$ and $c_x$, which are highlighted in bold. M, I and E represent morning, intermediate and evening types, respectively.